

NOWS: Neural Operator Warm Starts for Accelerating Iterative Solvers

Mohammad Sadegh Eshaghi¹, Cosmin Anitescu¹, Navid Valizadeh¹, Yizheng Wang³,
Xiaoying Zhuang¹, and Timon Rabczuk^{*2}

¹Chair of Computational Science and Simulation Technology, Institute of Photonics, Department of Mathematics and Physics, Leibniz University Hannover, 30167 Hannover, Germany

²Institute of Structural Mechanics, Bauhaus-Universität Weimar, Germany

³Department of Engineering Mechanics, Tsinghua University, Beijing, China

ABSTRACT

Partial differential equations (PDEs) underpin quantitative descriptions across the physical sciences and engineering, yet high-fidelity simulation remains a major computational bottleneck for many-query, real-time, and design tasks. Data-driven surrogates can be strikingly fast but are often unreliable when applied outside their training distribution. Here we introduce **Neural Operator Warm Starts (NOWS)**, a hybrid strategy that harnesses learned solution operators to accelerate classical iterative solvers by producing high-quality initial guesses for Krylov methods such as conjugate gradient and GMRES. NOWS leaves existing discretizations and solver infrastructures intact, integrating seamlessly with finite-difference, finite-element, isogeometric analysis, finite volume method, etc. Across our benchmarks, the learned initialization consistently reduces iteration counts and end-to-end runtime, resulting in a reduction of the computational time of up to 90%, while preserving the stability and convergence guarantees of the underlying numerical algorithms. By combining the rapid inference of neural operators with the rigor of traditional solvers, NOWS provides a practical and trustworthy approach to accelerate high-fidelity PDE simulations.

Introduction

From predicting the evolution of weather systems and modeling blood flow in the human body to designing aircraft and simulating the behavior of materials under stress, PDEs form the mathematical foundation of much of modern science and engineering. Advances in computational methods over the past half-century have made it possible to simulate increasingly complex systems with remarkable accuracy, transforming both fundamental research and industrial practice¹. Yet, the growing demand for high-fidelity models, driven by real-time and design tasks, and involving large numbers of degrees of freedom and intricate geometries, has pushed traditional numerical solvers to their computational limits². This challenge is particularly acute in applications such as optimization³, uncertainty quantification⁴, and digital twins^{5,6}, where even state-of-the-art algorithms can be prohibitively slow. Classical numerical methods, such as Finite Element Method (FEM), Finite Difference Method (FDM), and Finite Volume Method (FVM), combined with iterative solvers^{7–10} such as conjugate gradient^{11–13} or GMRES^{14–17}, remain the gold standard for robustness and accuracy. However, as the scale of problems grows, these solvers often require large numbers of iterations to converge, particularly for ill-conditioned systems¹⁸, or complex geometries¹⁹. High-resolution meshes further amplify the computational burden, making acceleration strategies increasingly essential²⁰.

In recent years, neural operators have emerged as a promising alternative by learning mappings between function spaces and approximating entire families of PDE solution operators. Early work includes the Graph Kernel Network²¹, which uses integral kernels implemented via graph message-passing. DeepONet²², inspired by the universal approximation theorem for operators, approaches the problem through a branch–trunk network decomposition, enabling flexible representation of nonlinear operators across diverse domains. The Fourier Neural Operator (FNO)²³ introduced spectral convolution layers to capture global dependencies, demonstrating strong performance on a range of parametric PDEs. Notably, the authors report FNO as the first ML-based method to successfully model turbulent flows with zero-shot super-resolution. The Variational Physics-informed Neural Operator (VINO)²⁴ further extends this framework by incorporating variational inference and physics-informed constraints, enabling robust learning in settings without any data. Variants based on transformers^{25–27} and graph neural networks²⁸ have extended these capabilities to irregular meshes²⁵, complex geometries²⁹, and coupled multi-physics systems^{30,31}. While these models often achieve inference speeds far exceeding classical solvers once trained, their training cost and limited robustness to distribution shifts remain significant challenges.

*Corresponding author. Email: timon.rabczuk@uni-weimar.de

Parallel to these developments, there is a growing body of work exploring hybrid methods that integrate learned surrogates with traditional numerical solvers. Neural networks have been employed to correct coarse-grid results in multigrid and solver-in-the-loop schemes³², to design improved iterative strategies with convergence guarantees^{33–35}, and to generate better initial guesses for nonlinear problems³⁶. They have also been used to construct problem-dependent prolongation and restriction operators^{37,38}, and to learn multigrid-augmented or data-driven preconditioners^{39–49}. While these approaches can significantly accelerate convergence by addressing low-frequency error components, they often require architectural modifications to the solver, may introduce stability concerns, and sometimes lack theoretical convergence guarantees. By contrast, the concept of using learned models purely for initialization, providing a warm start for iterative solvers, has received comparatively little attention, and where it has been examined⁵⁰, it has typically been restricted to specialized applications such as steady-state fluid simulations, without a systematic evaluation across PDE types, solver families, and parametric variations.

Here we introduce Neural Operator Warm Starts (NOWS), a hybrid paradigm that unites the speed of learned operators with the reliability of classical iterative solvers. Rather than replacing numerical methods, NOWS employs a neural operator to generate high-quality initial guesses that sharply reduce the initial residual, thereby lowering the iteration count required for full convergence. The neural operator rapidly eliminates the bulk of the error, leaving the classical solver to perform only fine-scale corrections. Crucially, this strategy preserves the stability, interpretability, and rigorous convergence guarantees of the underlying numerical method while leveraging the expressive power and speed of modern neural architectures. Because it requires no changes to the iterative scheme or preconditioning, NOWS is solver-agnostic and compatible with a wide range of existing solvers, including FEM, FDM, IGA, FVM, etc.

We demonstrate NOWS across diverse static and dynamic PDEs, showing iteration count reductions of two- to ten-fold and total runtime savings of 25–90%, without sacrificing accuracy or robustness. Comparative results against purely classical and purely neural approaches reveal that NOWS offers a distinctive balance of efficiency and reliability, performing well even under mesh variation and changes in domain geometry. This inversion of perspective, from substituting numerical methods to complementing them, bridges the gap between data-driven learning and physics-based computation. The resulting framework is broadly applicable in domains where PDEs are the computational bottleneck, including climate and geophysical modeling, biomedical simulation, structural engineering, and reactive flow design. More generally, NOWS illustrates a principled pathway for integrating machine learning into scientific computing, enhancing rather than supplanting the foundational strengths of traditional numerical methods.

Results

NOWS: Bridging Neural Operators and Iterative Solvers

We consider the generic family of parametric partial differential equations of the form

$$(L_a u)(x) = f(x), \quad x \in D, \quad u(x) = 0, \quad x \in \partial D, \quad (1)$$

for parameters $a \in \mathcal{A}$, right-hand side $f \in \mathcal{U}^*$, and a bounded domain $D \subset \mathbb{R}^d$. The solution $u : D \rightarrow \mathbb{R}$ is assumed to live in a Banach space \mathcal{U} , and the operator $L_a : \mathcal{A} \rightarrow \mathcal{L}(\mathcal{U}; \mathcal{U}^*)$ maps the parameter space into a space of linear operators from \mathcal{U} to its dual, \mathcal{U}^* . The solution operator naturally associated with this PDE is

$$\mathcal{G}^\dagger := L_a^{-1} f : \mathcal{A} \rightarrow \mathcal{U},$$

which maps the parameter a to the solution u . When needed, we assume that the domain D is discretized into $K \in \mathbb{N}$ points and that we observe $N \in \mathbb{N}$ pairs of coefficients and approximate solutions $\{a^{(i)}, u^{(i)}\}_{i=1}^N$, which are used for model training. Here, the coefficients $a^{(i)}$ are independent and identically distributed samples from a probability measure μ supported on \mathcal{A} , and the corresponding solutions $u^{(i)}$ are pushforward under \mathcal{G}^\dagger .

At the first stage, we train a neural operator offline. The training task is to approximate the map between two infinite-dimensional spaces using only a finite collection of input–output pairs, and possibly physical laws when the network is physics-informed. More concretely, let \mathcal{A} and \mathcal{U} denote Banach spaces of functions defined on bounded domains $D \subset \mathbb{R}^d$ and $D' \subset \mathbb{R}^{d'}$, respectively, and let $\mathcal{G}^\dagger : \mathcal{A} \rightarrow \mathcal{U}$ be the (possibly nonlinear) solution operator. Given observations $\{a^{(i)}, u^{(i)}\}_{i=1}^N$, where $a^{(i)} \sim \mu$ are drawn from a probability distribution on \mathcal{A} and $u^{(i)} = \mathcal{G}^\dagger(a^{(i)})$ are possibly corrupted by noise, the goal is to construct a parametric surrogate

$$\mathcal{G}_\theta : \mathcal{A} \rightarrow \mathcal{U}, \quad \theta \in \mathbb{R}^p, \quad (2)$$

and determine parameters $\theta^\dagger \in \mathbb{R}^p$ such that $\mathcal{G}_{\theta^\dagger} \approx \mathcal{G}^\dagger$. Neural operators such as FNO, DeepONet, VINO, and their extensions provide flexible frameworks for this approximation.

Once trained, the neural operator is integrated into the NOWS workflow (Fig. 1). The essential idea is simple: instead of relying on the neural operator for the entire solution process, we use it to provide an accurate initial guess for a conventional iterative solver. This initialization reduces the magnitude of the initial residual, allowing the solver to converge in significantly fewer iterations while maintaining its native guarantees of stability and accuracy. Crucially, the approach is solver-agnostic: any iterative scheme with any preconditioner, including conjugate gradient, GMRES, and multigrid methods, can be combined with NOWS. Similarly, the framework is independent of the underlying numerical discretization, and can be applied with finite element, finite difference, isogeometric, or finite volume methods.

The neural operator component of NOWS can be selected according to the problem’s requirements. Fourier Neural Operators are particularly well-suited for problems with periodic domains or smooth spectral structures, DeepONets offer flexibility across diverse geometries, and VINO integrates physics into loss functions, thereby enhancing generalization capability. Importantly, neural operators enjoy resolution invariance; models trained on coarse discretizations can be applied to finer meshes without retraining. This property allows us to train efficiently at modest resolution and later deploy the operator to accelerate solvers at scales where traditional training would be infeasible. We demonstrate this capability in the rising hot-smoke plume problem, where a neural operator trained on a coarse grid was successfully used to initialize solvers on high-resolution meshes, yielding consistent acceleration.

NOWS thus acts as a bridge between the speed of learned models and the reliability of numerical solvers. The neural operator eliminates the expensive early phase of iterative refinement, while the classical solver ensures full accuracy even under conditions not represented in the training set. The combination results in substantial runtime savings, robustness across problem classes, and seamless compatibility with established computational infrastructures. In the subsequent subsections, we will evaluate NOWS’s performance by through a range of numerical examples, covering various discretization methods and geometries.

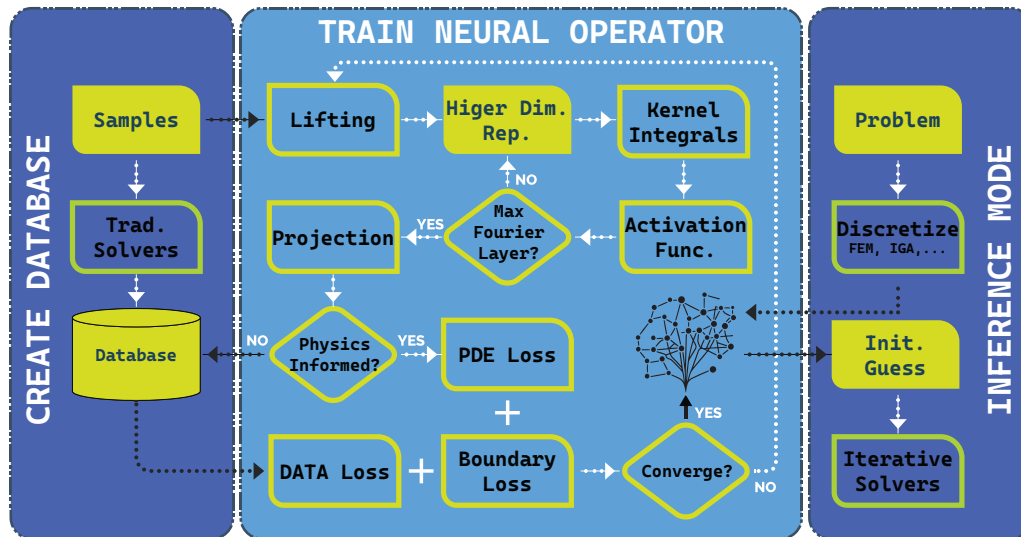


Fig. 1. Workflow of the Neural Operator Warm Start (NOWS) framework. Schematic overview of the NOWS methodology integrating neural operators and numerical solvers. The left branch illustrates the *data creation phase*, where data are generated, if needed (not for PI versions), using traditional solvers. The middle part describes *training phase*, where a Neural Operator is trained through a combination of data, physics, and boundary losses. The architecture cycles through lifting, integral kernels (Fourier layers), activation, and projection steps until convergence. The right branch shows the *inference phase*, in which parametric PDE problems are discretized (e.g., using FEM, IGA, FVM). The trained Neural Operator provides an initial guess for a conventional iterative solver (e.g., CG, GMRES), which then refines the solution to full numerical accuracy. This hybrid workflow leverages the efficiency of learned models and the robustness of classical solvers to accelerate PDE solvers.

Robustness of NOWS across resolutions

We first consider the canonical Poisson equation, a second-order elliptic PDE with a source term $p(x)$, given by

$$\begin{aligned} \nabla^2 s(x) + p(x) &= 0, & x \in \Omega &= [0, 1]^2, \\ s(x) &= 0, & x \in \partial\Omega, \end{aligned} \quad (3)$$

where the objective is to learn the solution operator \mathcal{G} that maps the source function $p(x)$ to the corresponding solution $s(x)$. To construct the neural operator, we trained a VINO using pairs $\{p(x), s(x)\}$ and PDE itself, where the forcing terms $p(x)$ are generated from Gaussian random fields (GRFs). The trained operator serves as the initialization mechanism in the NOWS framework. Once training is complete, we evaluate the method on 2000 previously unseen realizations of $p(x)$. For the iterative solver, we employ the conjugate gradient (CG) method, chosen for its efficiency in handling symmetric positive-definite systems arising from discretizations of the Poisson problem.

The experiments are conducted independently at multiple mesh resolutions, ranging from coarse to high-fidelity discretizations. This design allows us to assess the performance of NOWS across discretization scales, demonstrating that the method consistently delivers effective initializations and accelerates convergence regardless of mesh density. Figure 2 summarizes the performance of NOWS compared with the standalone iterative solver over the 2000 test cases. Across all resolutions, NOWS achieves a consistent reduction in iteration counts and total runtime while retaining the final accuracy of the classical solver. The results confirm that using a neural operator solely for initialization provides a reliable and scalable acceleration strategy for elliptic PDEs.

The results in Fig. 2 illustrate the impact of NOWS across four discretization levels, ranging from coarse meshes (64×64) to high-fidelity grids (512×512). Each row corresponds to a specific resolution, with the left column reporting the relative tolerance versus iteration count, and the right column summarizing the runtime to convergence across the 2000 test cases. The gradient arrow on the left highlights the transition from coarse discretizations at the top to high-fidelity meshes at the bottom, providing a visual link between mesh density and solver behavior.

In all cases, the conjugate gradient (CG) method initialized with NOWS (blue) consistently outperforms the standalone CG solver (orange). The left panels clearly show that NOWS reduces the initial residual magnitude, shifting the convergence curve downward and resulting in faster attainment of target tolerances. This improvement translates directly into reduced iteration counts: at coarse resolution, savings of roughly 30%–40% are observed, while for finer meshes the savings become even more pronounced, exceeding 50% in many cases.

The right panels quantify these improvements in terms of runtime. Across all resolutions, the violin plots indicate both lower mean solution times and reduced variance for NOWS compared with CG. The annotated percentages on the right axis represent the fraction of computational time saved by NOWS, demonstrating robust acceleration benefits that persist even as the problem size grows. Importantly, the advantage of NOWS scales favorably with resolution: as mesh density increases, the gap between the two methods widens, underscoring the resolution-invariance property of neural operators.

Together, these results confirm that NOWS provides reliable acceleration across discretization levels, delivering substantial iteration and runtime savings without compromising accuracy. This robustness with respect to mesh resolution is critical for practical applications, where simulations often demand high fidelity but cannot afford the prohibitive computational cost of classical iterative refinement alone.

Physics-Informed NOWS

We evaluate the role of physics-informed supervision in training neural operators for steady-state Darcy flow. The benchmark problem involves two-dimensional subsurface flow through heterogeneous porous media, where the conductivity field $p(x)$ is modeled as a piecewise-constant random function and the hydraulic head $s(x)$ satisfies

$$-\nabla \cdot (p(x)\nabla s(x)) = f(x), \quad x \in [0, 1]^2, \quad s(x) = 0, \quad x \in \partial[0, 1]^2, \quad (4)$$

with $f(x) = 1$. The objective is to learn the operator $\mathcal{G} : p \mapsto s$, mapping the heterogeneous conductivity field to the solution of the PDE. Although the PDE is linear, the solution operator is inherently nonlinear due to the piecewise nature of $p(x)$.

To enforce physics consistency, the neural operator is trained via the variational (energy) form of the Darcy equation, minimizing the corresponding functional derived from the PDE. Three training strategies are compared: purely data-driven supervision, physics-informed training based on the variational residual, and a hybrid approach combining data and physics losses. The operator is coupled with a classical finite element method (FEM) solver in this study, providing a reference solution for error evaluation; this contrasts with previous experiments using finite difference discretizations. All models share the same backbone structure and are trained on permeability fields drawn from Gaussian random processes with varying correlation lengths.

Figure 3a demonstrates that the physics-informed neural operator achieves the most robust generalization. As the number of Fourier modes or network parameters increases, the test error decreases under physics-only supervision, while it rises for

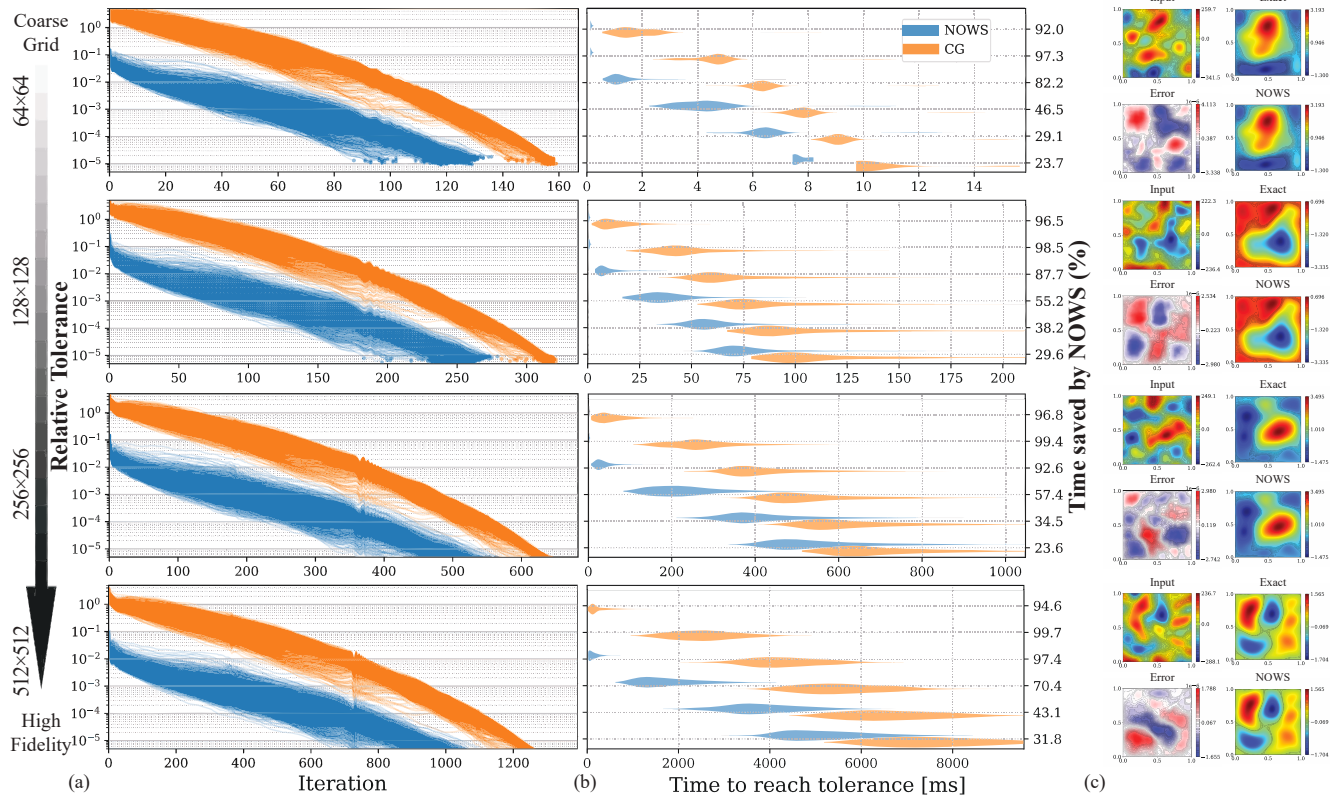


Fig. 2. NOWS accelerates iterative solvers in various resolutions. (a) Overlaid residual-vs-iteration trajectories for the two methods on the 2000-sample test set, showing that NOWS reduces both the initial residual and the number of iterations to convergence. (b) Violin plots of wall-clock time distributions (per test instance) required to reach several relative residual tolerances, comparing the baseline and NOWS. (c) An example test case comparing the NOWS solution, the reference obtained with the direct solver. The NOWS removes the large-scale error, while the classical solver enforces exactness. Results are aggregated over 2000 unseen GRF realizations.

data-only and mixed models, indicating susceptibility to overfitting in the absence of explicit PDE constraints. Embedding the PDE structure directly in the training loss produces smoother, more stable operator predictions that respect the underlying physics across resolution scales and heterogeneous permeability contrasts.

These results highlight that the incorporation of variational PDE constraints enables neural operators to capture essential physical structure, improving both predictive accuracy and robustness. The synergy between energy-based loss formulations and classical FEM solutions establishes a framework for physics-consistent operator learning that is both generalizable and compatible with established numerical methods. Embedding the underlying physics reduces the reliance on large labeled datasets and promotes smoother, more stable operator learning, which are key characteristics for PDE acceleration within the NOWS framework.

Preconditioning of Krylov Methods in NOWS

We next assess the performance of NOWS framework when integrated with various preconditioning techniques for Krylov subspace methods. The analysis is carried out on the steady-state Darcy flow problem, using VINO via the variational (energy-based) formulation of the governing PDE. In this configuration, the neural operator provides physics-consistent initial conditions for the iterative solver.

To investigate the interplay between data-driven initialization and algebraic preconditioning, we consider several standard preconditioners for the conjugate gradient (CG) method, including the unpreconditioned baseline, Jacobi, SSOR (Symmetric Successive Over-Relaxation), ICC (Incomplete Cholesky), and ILU (Incomplete LU) schemes. Each preconditioner alters the spectral characteristics of the discrete Darcy system and thereby affects convergence behavior.

For each configuration, we compare the baseline CG solver with its NOWS-augmented counterpart, in which the neural operator prediction serves as the initial iterate u_0 . Performance is evaluated over a range of relative residual tolerances, and both

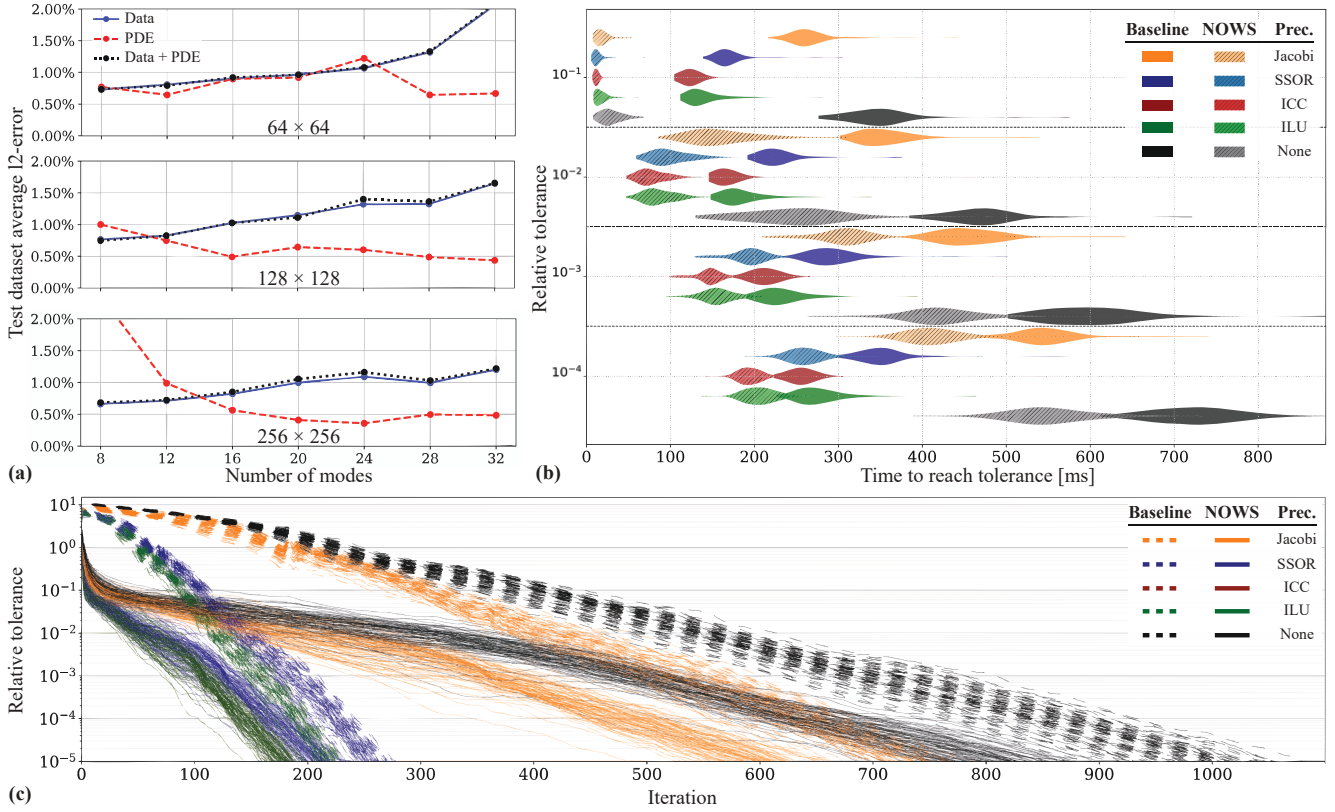


Fig. 3. Impact of physics-informed training and neural-operator warm starts (NOWS) on Darcy flow simulations. (a) Test error as a function of network complexity, comparing data-only, physics-only, and hybrid training strategies. Physics-informed supervision yields the most robust generalization, with test error decreasing as the number of Fourier modes or network parameters increases, whereas data-only and hybrid approaches exhibit overfitting. Embedding the PDE directly in the loss produces smoother and more stable operator predictions that respect the underlying physics across resolutions and heterogeneous permeability contrasts. (b) Wall-clock runtime distributions for various preconditioners and relative tolerance levels, with and without NOWS initialization. Across all preconditioners, NOWS consistently reduces solver runtime, demonstrating measurable acceleration even for simple Jacobi preconditioning, with more pronounced improvements for ICC and ILU schemes. (c) Relative residuals versus iteration count for different preconditioners. NOWS systematically lowers the initial residual and reduces the number of iterations required to achieve the prescribed convergence tolerance, illustrating solver-agnostic acceleration and robustness across preconditioning strategies.

iteration count and total runtime are recorded. The experiments are conducted across 2000 unseen permeability realizations, ensuring statistical robustness.

Figure 3b summarizes the runtime distributions for different preconditioners and tolerance levels, with and without NOWS initialization. Across all settings, a consistent pattern emerges: NOWS reduces solver runtime irrespective of the preconditioner employed. Even for simple diagonal preconditioners such as Jacobi, a measurable reduction in computational cost is observed, while more advanced schemes like ICC and ILU exhibit pronounced acceleration when combined with neural initialization.

The complementary nature of preconditioning and NOWS is further evident in Figure 3c, which reports the relative residuals as a function of iteration count. The NOWS initialization systematically decreases both the initial residual magnitude and the number of iterations required to meet the prescribed convergence criterion. This effect remains consistent across all preconditioners, demonstrating the robustness and solver-agnostic character of NOWS.

The results establish that the benefits of neural initialization are invariant to preconditioner selection. Regardless of the underlying conditioning strategy, the integration of NOWS accelerates convergence and reduces total runtime without modifying the solver’s structure. The neural operator provides a physically consistent approximation that narrows the solution search space, while preconditioners refine the spectral properties of the linear system. The preconditioning analysis thus reinforces the generality of NOWS as a physics-grounded, solver-independent enhancement for PDE computations.

Applicability to irregular geometries and Isogeometric Analysis

To demonstrate the flexibility of NOWS in complex domains, we consider a two-dimensional plate with arbitrarily shaped internal voids. The plate is modeled using a parametric linear elasticity problem, discretized with an isogeometric analysis (IGA) solver, where the displacement field $\mathbf{u}(x, y)$ satisfies

$$\begin{aligned} \frac{\partial \sigma_{xx}}{\partial x} + \frac{\partial \sigma_{xy}}{\partial y} + f_x &= 0, \\ \frac{\partial \sigma_{yx}}{\partial x} + \frac{\partial \sigma_{yy}}{\partial y} + f_y &= 0, \\ \mathbf{u}(x, y) &= 0 \quad \text{for } x = 0, L, \\ \boldsymbol{\sigma} \cdot \mathbf{n} &= \hat{\mathbf{t}}(y) \quad \text{for } y = D, \end{aligned} \tag{5}$$

with stress defined via the constitutive relation $\boldsymbol{\sigma} = \mathbf{E} \mathbf{D} \boldsymbol{\varepsilon}$. Here, E denotes the spatially varying elasticity modulus, \mathbf{D} is the plane-stress constitutive matrix, and $\boldsymbol{\varepsilon}$ is the strain vector. The matrix \mathbf{D} and vector definitions are given by

$$\mathbf{D} = \frac{1}{1 - \nu^2} \begin{bmatrix} 1 & \nu & 0 \\ \nu & 1 & 0 \\ 0 & 0 & \frac{1-\nu}{2} \end{bmatrix}, \tag{6}$$

$$\boldsymbol{\sigma} = [\sigma_{xx}, \sigma_{yy}, \sigma_{xy}]^T, \quad \boldsymbol{\varepsilon} = [\varepsilon_{xx}, \varepsilon_{yy}, \varepsilon_{xy}]^T. \tag{7}$$

The domain $\Omega_p = [0, 5]^2 \setminus \mathcal{V}$ is parameterized by a set of design parameters $p \in \mathcal{P}$, where \mathcal{V} represents the collection of arbitrary holes within the central region $[1, 4]^2$. Dirichlet boundary conditions are imposed on the left edge, and a constant traction is applied on the right edge. The neural operator is trained to approximate the mapping $\mathcal{G} : \Omega_p \mapsto \mathbf{u}$, capturing the solution field across variable geometries.

Random samples of allowable domain configurations are illustrated in Figure 4a. The CG solver is initialized either from zero or using the neural operator prediction, NOWS. The results in Figure 4 summarize the performance of NOWS for 50 random test instances. Relative residuals versus iteration count (Fig. 4b) and wall-clock runtime to convergence (Fig. 4c) clearly demonstrate the acceleration benefits.

Across all geometries, NOWS consistently reduces the initial residual magnitude, lowering the convergence curve and enabling faster attainment of target tolerances. This improvement corresponds to a reduction of approximately 90% in iteration counts and yields a speed-up of roughly tenfold in runtime. The annotated percentages in Fig. 4c indicate the fraction of computational time saved, highlighting the robustness of NOWS even as the domain complexity increases.

These results confirm that NOWS effectively accelerates iterative solvers for IGA-based simulations on irregular domains, providing substantial savings in both iterations and runtime without compromising solution accuracy.

Applicability to dynamic problems

To evaluate the generalization and robustness of NOWS in time-dependent settings, we apply the framework to the one-dimensional viscous Burgers' equation, a canonical nonlinear PDE that models one-dimensional fluid motion under diffusion and advection. The governing equation is

$$\partial_t u(x, t) + \partial_x \left(\frac{u^2(x, t)}{2} \right) = \nu \partial_{xx} u(x, t), \quad x \in (0, 1), t \in (0, 1], \tag{8}$$

subject to periodic boundary conditions and an initial condition $u(x, 0) = u_0(x)$, where $u_0 \in L^2_{\text{per}}((0, 1); \mathbb{R})$ and $\nu > 0$ is the viscosity. The objective is to learn the nonlinear operator

$$\mathcal{G}^\dagger : L^2_{\text{per}}((0, 1); \mathbb{R}) \rightarrow H^1_{\text{per}}((0, 1); \mathbb{R}), \quad u_0 \mapsto u(\cdot, t), \tag{9}$$

which maps the initial field to the solution at later times within the time interval $[0, 1]$.

In this experiment, NOWS is coupled with a classical finite-difference solver accelerated using the CG method, and we have used Multi-Head Neural Operator (MHNO)⁵¹ for operator learning. Figure 5a illustrates the representative input profile, the corresponding exact and NOWS-predicted solutions, and their pointwise difference. The runtime statistics, summarized in Figure 5b, confirm the efficiency gains provided by NOWS. The average wall-clock time per solve decreases from 9.62 s for the baseline CG method to 4.75 s with NOWS initialization—corresponding to approximately **50% time savings**. Detailed statistics indicate consistent acceleration across all test cases, with mean, median, minimum, and maximum time reductions of 50.5%, 50.9%, 41.7%, and 52.8%, respectively. These results demonstrate that NOWS generalizes effectively to nonlinear, transient problems and retains its acceleration capability in dynamic PDE settings.

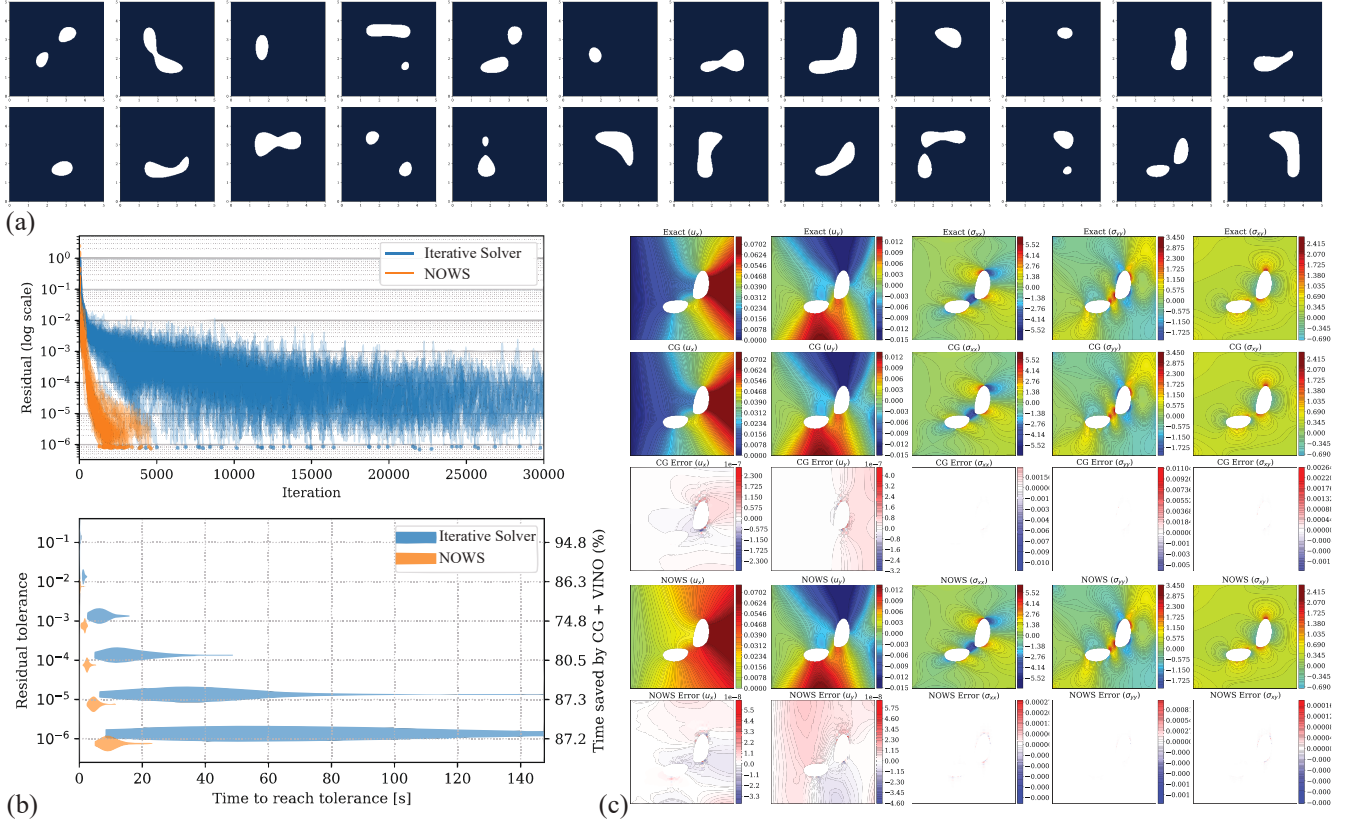


Fig. 4. NOWS accelerates the iterative solution of PDEs on irregular domains. (a) Random samples of allowable domain configurations with arbitrary voids. The plate is clamped on the left edge and subjected to constant traction on the right edge. (b) Relative residuals versus iteration count for the conjugate gradient (CG) solver initialized from zero or using the neural operator warm start (NOWS). NOWS consistently reduces the initial residual magnitude, lowering the convergence curve and decreasing the number of iterations required to reach the target tolerance. (c) Wall-clock runtime to convergence for 50 test instances. Across all geometries, NOWS yields 10-fold speed-up and reduces iteration counts by roughly 90%. Annotated percentages indicate the fraction of computational time saved, demonstrating robust acceleration benefits even for complex domain configurations.

Smoke Plume – Resolution Invariance

To further assess the scalability and generalization of NOWS, we consider a coupled, nonlinear flow problem governed by the incompressible Navier–Stokes equations with buoyancy-driven smoke transport. The system is representative of large-scale multiphysics simulations typically solved using the FVM. The governing equations are

$$\nabla \cdot \mathbf{u} = 0, \quad (10)$$

$$\frac{\partial \mathbf{u}}{\partial t} + (\mathbf{u} \cdot \nabla) \mathbf{u} = -\nabla p + \nu \nabla^2 \mathbf{u} + \mathbf{g} \beta (\rho - \rho_0), \quad (11)$$

$$\frac{\partial \rho}{\partial t} + (\mathbf{u} \cdot \nabla) \rho = D \nabla^2 \rho, \quad (12)$$

where \mathbf{u} denotes velocity, p the pressure, ρ the smoke density, ν the kinematic viscosity, β the buoyancy coefficient, and D the diffusion coefficient. The system couples the smoke advection–diffusion process with incompressible fluid motion, and the pressure projection step is solved iteratively using a CG solver.

In this setting, NOWS is employed to provide initial guesses for the CG-based pressure projection at each simulation step, thereby accelerating convergence while maintaining physical fidelity. The underlying numerical scheme follows a semi-Lagrangian advection and buoyancy update, followed by a pressure correction step enforcing incompressibility. The training process in NOWS ensures that the learned operator generalizes across flow configurations without requiring retraining for each grid.

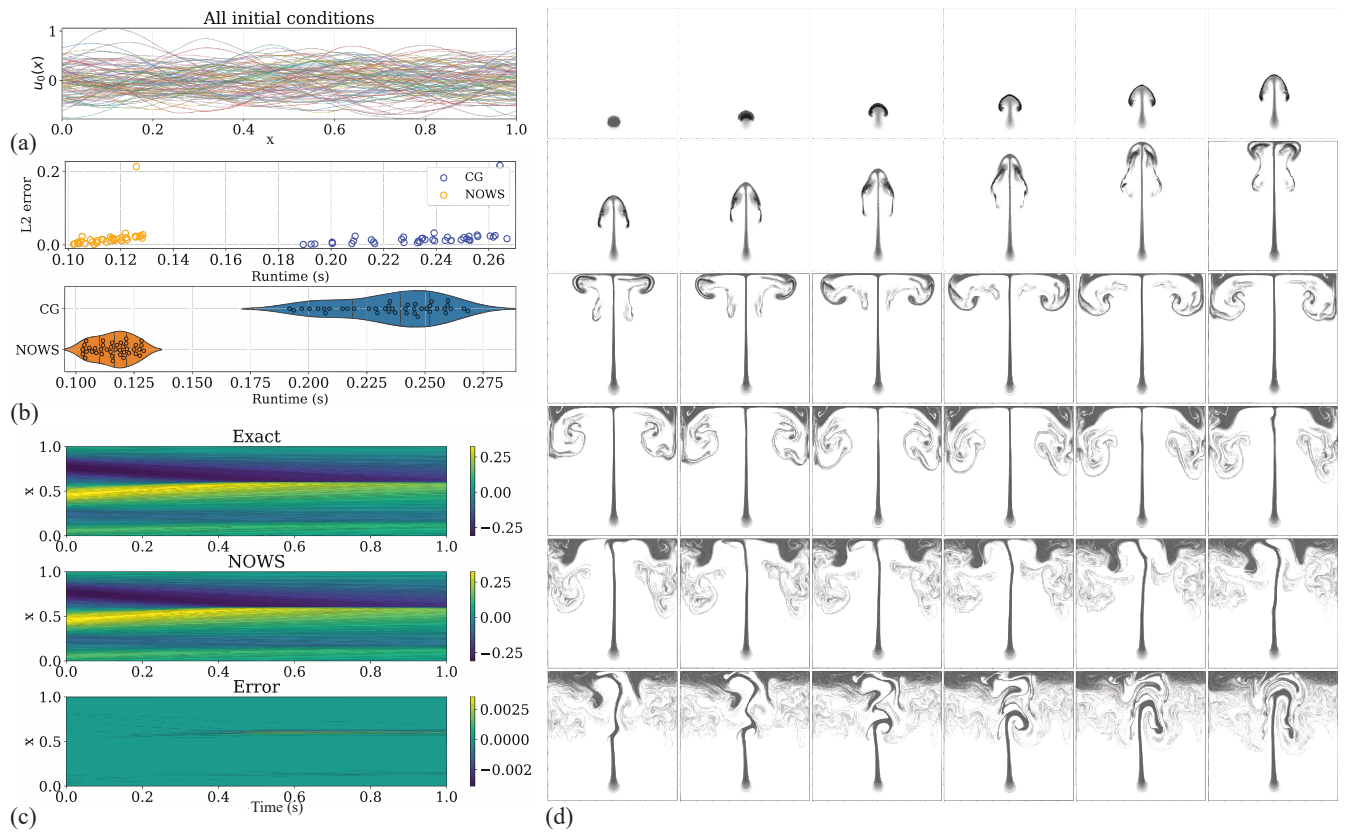


Fig. 5. NOWS for dynamic problems (a) Ensemble of initial conditions in the test dataset used for the Burgers' equation. (b) Comparing runtime distributions of CG and NOWS: scatter plot of runtime versus L_2 error for each sample (top), violin plots comparing the runtime distributions of the CG and NOWS solvers (bottom). (c) Spatiotemporal evolution of the solution filed for a representative test sample in the Burgers' equation: exact reference (top), NOWS result (middle), and the corresponding error field (bottom). (d) **Resolution-invariant acceleration of coupled fluid–smoke simulations using NOWS.** A rising smoke plume governed by buoyancy-driven Navier–Stokes dynamics is simulated using NOWS. The neural operator, trained on coarse 64×64 grids, is applied directly to 256×256 simulations without retraining. Shown are representative smoke density snapshots at multiple time steps, illustrating stable and accurate evolution. The NOWS initialization reduces total solver iterations by over 70% and accelerates runtime by a factor of three, confirming robust resolution-invariant generalization across grid scales.

To examine the mesh resolution invariance of NOWS, the neural operator was trained exclusively on coarse-grid simulations (64×64) and directly deployed on high-resolution grids (256×256) without further fine-tuning. The network has been trained to predict the pressure field at the current time step from the pressure field from the previous time step. Remarkably, the coarse-trained model provided physically consistent initializations for the fine-grid solver, retaining accuracy while significantly accelerating convergence. Quantitative performance comparisons highlight the impact of neural initialization. Without NOWS, the solver required 69,703 total iterations across 150 successful runs, yielding an average runtime of 294.74 s. When initialized with NOWS, total iterations reduced to 17,438, corresponding to a mean runtime of 93.85 s—an overall reduction of approximately **68%** in computational time. Notably, convergence was achieved in all cases, indicating that the neural initialization preserves solver stability while enhancing efficiency.

Figure 5 illustrates representative smoke density fields at various time steps. The rising hot plume demonstrates that NOWS enables rapid convergence even for large-scale coupled PDE systems. The resolution-invariant behavior further confirms the ability of NOWS to generalize across spatial discretizations, a crucial property for scientific computing workflows where mesh adaptivity or refinement is required. The integration of NOWS with the finite volume solver thus represents a scalable strategy for accelerating multiphysics simulations without compromising physical accuracy.

Discussion

The results presented across diverse PDE systems demonstrate that the NOWS framework provides a broadly applicable and robust acceleration mechanism for numerical solvers. By learning problem-specific operator mappings that approximate the inverse of the governing equations, NOWS delivers accurate initializations that significantly reduce the computational cost of iterative schemes. This hybridization between classical numerical methods and machine learning yields several key insights and implications.

First, the empirical evidence confirms that the physics-informed training of neural operators leads to superior generalization compared with purely data-driven approaches. In the Darcy flow experiments, enforcing the variational energy of the PDE during training resulted in models that remained stable and resistant to overfitting, even as network capacity or Fourier mode count increased. Using a physics-based loss function ensures that the network adheres to conservation laws and boundary constraints, maintaining fidelity across unseen material configurations and discretization scales.

Second, coupling NOWS with standard Krylov subspace preconditioner establishes a flexible and solver-agnostic framework. Across all examined preconditioners—from simple Jacobi to incomplete factorizations such as ICC and ILU—the neural warm start consistently lowered the initial residual and reduced iteration counts by up to an order of magnitude. These benefits are achieved without altering the solver’s mathematical formulation or convergence guarantees, distinguishing NOWS from traditional learned-solver replacements that may sacrifice interpretability or robustness.

Third, the integration of NOWS with Finite Difference, Finite Element, IGA, and Finite Volume frameworks highlights its modularity. The smoke plume experiment illustrates the resolution-invariance of the learned operator: a model trained on a coarse grid directly generalized to a four-times finer mesh without retraining, maintaining accuracy and achieving a threefold speed-up. This capability is particularly relevant for multiscale simulations and adaptive mesh refinement, where solver warm starts must remain consistent across varying resolutions.

Beyond raw performance, NOWS changes how machine learning can interact with physics-based computation. Rather than substituting classical solvers, the framework augments them, retaining deterministic convergence while learning efficient priors from data or physical principles. This paradigm offers a pragmatic path toward physics-aware scientific computing, enabling acceleration and scalability without compromising trustworthiness. Future research directions include extending NOWS to graph-based operator architectures for unstructured meshes and integrating uncertainty quantification to assess confidence in neural initializations. Collectively, these results position NOWS as a unifying approach for embedding machine learning into numerical solvers, bridging the gap between data-driven models and first-principles computation.

Method

Neural Operator Warm Starts (NOWS)

The proposed NOWS framework accelerates iterative PDE solvers by providing high-quality initial guesses derived from learned operator approximations. Rather than replacing classical numerical solvers, NOWS complements them by supplying accurate initializations that significantly reduce the number of iterations required for convergence.

Formally, given a PDE operator $\mathcal{L}(u; \theta) = f$ and its solution $u^* = \mathcal{L}^{-1}(f)$, a neural operator \mathcal{G}_ϕ is trained to approximate \mathcal{L}^{-1} from representative training data. At inference, $\mathcal{G}_\phi(f)$ serves as a warm start for the iterative solver:

$$u_0 = \mathcal{G}_\phi(f), \quad u_{k+1} = u_k + \alpha_k P^{-1}(f - \mathcal{L}(u_k)), \quad (13)$$

where P denotes a preconditioner and α_k the step size. This hybrid initialization enables rapid convergence while preserving the exactness of the final solution as determined by the classical solver.

In physics-informed configurations, the energy-based loss function provides physics-consistent training without requiring labeled data:

$$\mathcal{L}(\phi) = \frac{1}{|\mathcal{B}|} \sum_{(P,F,b) \in \mathcal{B}} |\Psi(\mathcal{G}_\phi(P,F,b); P,b) - \Psi_{\text{ref}}|, \quad (14)$$

where \mathcal{B} is a batch of training examples, Ψ_{ref} is a reference energy (often zero for equilibrium problems),.

Krylov Methods

Krylov subspace methods are widely used for the iterative solution of large sparse linear systems arising from PDE discretizations. Given a system $Au = b$, Krylov solvers such as the Conjugate Gradient (CG) and Generalized Minimal Residual (GMRES) methods build successive approximations in the subspace $\mathcal{K}_k(A, r_0) = \text{span}\{r_0, Ar_0, \dots, A^{k-1}r_0\}$, where $r_0 = b - Au_0$ is the initial residual. Their convergence rate depends on the spectral properties of A , which are often improved through preconditioning. Common preconditioners include Jacobi, Symmetric Successive Over-Relaxation (SSOR), Incomplete Cholesky (ICC), and Incomplete LU (ILU) factorization.

In this work, Nows provides an effective initialization for Krylov methods, thereby reducing the norm of the initial residual and accelerating convergence regardless of preconditioning. The synergy between neural warm starts and Krylov subspace acceleration offers consistent runtime reductions and robustness across linear and nonlinear PDE systems.

Numerical Solver

All PDEs considered in this study are discretized using standard numerical methods appropriate to their physical and geometrical characteristics. The Poisson equation is discretized using Finite Difference (FD) and the Darcy flow equation is discretized with Finite Element (FE) formulations, while the elasticity and plate problems are solved using Isogeometric Analysis (IGA). The smoke plume problem is simulated using a Finite Volume Method, which allows the coupling of advective transport and incompressible fluid dynamics through a pressure projection step. The underlying solvers are iterative, relying primarily on CG for symmetric positive-definite systems, with relative tolerance thresholds ranging from 10^{-3} to 10^{-6} depending on the case. Each solver configuration is benchmarked both with and without neural initialization. For consistency, all runs employ identical discretizations, boundary conditions, and stopping criteria. Timing and convergence statistics are averaged across multiple random realizations to ensure robustness of the performance assessment.

Data availability

The paper's datasets were created using the accompanying code. The dataset is available for free access at <https://github.com/eshaghi-ms/NOWS>

Code availability

The code for all numerical experiments is publicly accessible on GitHub at <https://github.com/eshaghi-ms/NOWS>.

References

1. Quarteroni, A. & Valli, A. *Numerical approximation of partial differential equations* (Springer, 1994).
2. Menghal, P. & Laxmi, A. J. Real time simulation: Recent progress & challenges. In *2012 International Conference on Power, Signals, Controls and Computation*, 1–6 (IEEE, 2012).
3. Biegler, L. T. *Nonlinear programming: concepts, algorithms, and applications to chemical processes* (SIAM, 2010).
4. Smith, R. C. *Uncertainty quantification: theory, implementation, and applications* (SIAM, 2024).
5. Fuller, A., Fan, Z., Day, C. & Barlow, C. Digital twin: enabling technologies, challenges and open research. *IEEE access* **8**, 108952–108971 (2020).
6. Es-haghi, M. S., Anitescu, C. & Rabczuk, T. Methods for enabling real-time analysis in digital twins: A literature review. *Computers & Structures* **297**, 107342 (2024).
7. Hageman, L. A. & Young, D. M. *Applied iterative methods* (Courier Corporation, 2012).
8. Greenbaum, A. *Iterative methods for solving linear systems* (SIAM, 1997).
9. Van der Vorst, H. A. *Iterative Krylov methods for large linear systems*. 13 (Cambridge University Press, 2003).
10. Xu, J. Iterative methods by space decomposition and subspace correction. *SIAM Review* **34**, 581–613 (1992). Available at <https://doi.org/10.1137/1034116>. <https://doi.org/10.1137/1034116>.
11. Kawata, S. & Nalcioglu, O. Constrained iterative reconstruction by the conjugate gradient method. *IEEE Transactions on Medical Imaging* **4**, 65–71 (1985).
12. Kershaw, D. S. The incomplete cholesky—conjugate gradient method for the iterative solution of systems of linear equations. *Journal of Computational Physics* **26**, 43–65 (1978). Available at <https://www.sciencedirect.com/science/article/pii/0021999178900980>.
13. Strandén, I. & Lidauer, M. Solving large mixed linear models using preconditioned conjugate gradient iteration. *Journal of Dairy Science* **82**, 2779–2787 (1999).
14. Kalantzis, V. *et al.* Solving sparse linear systems via flexible gmres with in-memory analog preconditioning. In *2023 IEEE High Performance Extreme Computing Conference (HPEC)*, 1–7 (2023).
15. Lindquist, N., Luszczek, P. & Dongarra, J. Accelerating restarted gmres with mixed precision arithmetic. *IEEE Transactions on Parallel and Distributed Systems* **33**, 1027–1037 (2022).
16. Thomas, S., Carson, E., Rozložník, M., Carr, A. & Świrydowicz, K. Iterated gauss–seidel gmres. *SIAM Journal on Scientific Computing* **46**, S254–S279 (2024). Available at <https://doi.org/10.1137/22M1491241>. <https://doi.org/10.1137/22M1491241>.

17. Amestoy, P. *et al.* Five-precision gmres-based iterative refinement. *SIAM Journal on Matrix Analysis and Applications* **45**, 529–552 (2024). Available at <https://doi.org/10.1137/23M1549079>. <https://doi.org/10.1137/23M1549079>.
18. Qiu, Y., Van Gijzen, M. B., Van Wingerden, J.-W., Verhaegen, M. & Vuik, C. Efficient preconditioners for pde-constrained optimization problems with a multi-level sequentially semi-separable matrix structure. *Electronic Transactions on Numerical Analysis* **44**, 3 (2015).
19. Mahesh, K., Constantinescu, G. & Moin, P. A numerical method for large-eddy simulation in complex geometries. *Journal of Computational Physics* **197**, 215–240 (2004).
20. Kronbichler, M. & Kormann, K. A generic interface for parallel cell-based finite element operator application. *Computers & Fluids* **63**, 135–147 (2012).
21. Li, Z. *et al.* Neural operator: Graph kernel network for partial differential equations. *arXiv preprint arXiv:2003.03485* (2020).
22. Lu, L., Jin, P., Pang, G., Zhang, Z. & Karniadakis, G. E. Learning nonlinear operators via deeponet based on the universal approximation theorem of operators. *Nature Machine Intelligence* **3**, 218–229 (2021).
23. Li, Z. *et al.* Fourier neural operator for parametric partial differential equations. *arXiv preprint arXiv:2010.08895* (2020).
24. Eshaghi, M. S. *et al.* Variational physics-informed neural operator (vino) for solving partial differential equations. *Computer Methods in Applied Mechanics and Engineering* **437**, 117785 (2025).
25. Hao, Z. *et al.* GNOT: A general neural operator transformer for operator learning. In Krause, A. *et al.* (eds.) *Proceedings of the 40th International Conference on Machine Learning*, vol. 202 of *Proceedings of Machine Learning Research*, 12556–12569 (PMLR, 2023). Available at <https://proceedings.mlr.press/v202/hao23c.html>.
26. Shih, B., Peyvan, A., Zhang, Z. & Karniadakis, G. E. Transformers as neural operators for solutions of differential equations with finite regularity. *Computer Methods in Applied Mechanics and Engineering* **434**, 117560 (2025). Available at <https://www.sciencedirect.com/science/article/pii/S0045782524008144>.
27. Guibas, J. *et al.* Adaptive fourier neural operators: Efficient token mixers for transformers. *arXiv preprint arXiv:2111.13587* (2021).
28. Xu, M. *et al.* Equivariant graph neural operator for modeling 3d dynamics. *arXiv preprint arXiv:2401.11037* (2024).
29. Fu, X. *et al.* Spatio-temporal neural operator on complex geometries. *Computer Physics Communications* **315**, 109754 (2025). Available at <https://www.sciencedirect.com/science/article/pii/S0010465525002565>.
30. Zheng, H. & Lin, G. Multi-fidelity prediction and uncertainty quantification with laplace neural operators for parametric partial differential equations. *arXiv preprint arXiv:2502.00550* (2025).
31. Li, S., Wang, T., Sun, Y. & Tang, H. Multi-physics simulations via coupled fourier neural operator. *arXiv preprint arXiv:2501.17296* (2025).
32. Um, K., Brand, R., Fei, Y. R., Holl, P. & Thuerey, N. Solver-in-the-loop: Learning from differentiable physics to interact with iterative pde-solvers. *Advances in neural information processing systems* **33**, 6111–6122 (2020).
33. Hsieh, J.-T., Zhao, S., Eismann, S., Mirabella, L. & Ermon, S. Learning neural pde solvers with convergence guarantees. *arXiv preprint arXiv:1906.01200* (2019).
34. He, J. & Xu, J. Mgnet: A unified framework of multigrid and convolutional neural network. *Science china mathematics* **62**, 1331–1354 (2019).
35. Chen, Y., Dong, B. & Xu, J. Meta-mgnet: Meta multigrid networks for solving parameterized partial differential equations. *Journal of computational physics* **455**, 110996 (2022).
36. Huang, J., Wang, H. & Yang, H. Int-deep: A deep learning initialized iterative method for nonlinear problems. *Journal of computational physics* **419**, 109675 (2020).
37. Luz, I., Galun, M., Maron, H., Basri, R. & Yavneh, I. Learning algebraic multigrid using graph neural networks. In III, H. D. & Singh, A. (eds.) *Proceedings of the 37th International Conference on Machine Learning*, vol. 119 of *Proceedings of Machine Learning Research*, 6489–6499 (PMLR, 2020). Available at <https://proceedings.mlr.press/v119/luz20a.html>.

38. Greenfeld, D., Galun, M., Basri, R., Yavneh, I. & Kimmel, R. Learning to optimize multigrid PDE solvers. In Chaudhuri, K. & Salakhutdinov, R. (eds.) *Proceedings of the 36th International Conference on Machine Learning*, vol. 97 of *Proceedings of Machine Learning Research*, 2415–2423 (PMLR, 2019). Available at <https://proceedings.mlr.press/v97/greenfeld19a.html>.
39. Azulay, Y. & Treister, E. Multigrid-augmented deep learning preconditioners for the helmholtz equation. *SIAM Journal on Scientific Computing* **45**, S127–S151 (2022).
40. Tan, S., Miao, K., Edelman, A. & Rackauckas, C. Scalable higher-order nonlinear solvers via higher-order automatic differentiation. *arXiv preprint arXiv:2501.16895* (2025).
41. Lee, Y. *et al.* Fast meta-solvers for 3d complex-shape scatterers using neural operators trained on a non-scattering problem. *Computer Methods in Applied Mechanics and Engineering* **446**, 118231 (2025).
42. Herb, J. & Fritzen, F. Accelerating conjugate gradient solvers for homogenization problems with unitary neural operators. *arXiv preprint arXiv:2508.02681* (2025).
43. Giraud, L., Kruse, C., Mycek, P., Shpakovych, M. & Xiang, Y. *Neural network preconditioning: a case study for the solution of the parametric Helmholtz equation*. Ph.D. thesis, Inria Centre at the University of Bordeaux, France (2025). Available at <https://hal.science/hal-05157038>.
44. Zhang, E. *et al.* Blending neural operators and relaxation methods in pde numerical solvers. *Nature Machine Intelligence* **6**, 1303–1313 (2024).
45. Han, X., Hou, F. & Qin, H. Ugrid: An efficient-and-rigorous neural multigrid solver for linear pdes. *arXiv preprint arXiv:2408.04846* (2024).
46. Huang, R., Chang, K., He, H., Li, R. & Xi, Y. Reducing operator complexity in algebraic multigrid with machine learning approaches. *arXiv preprint arXiv:2307.07695* (2023).
47. Kopaničáková, A., Lee, Y. & Karniadakis, G. E. Leveraging operator learning to accelerate convergence of the preconditioned conjugate gradient method. *arXiv preprint arXiv:2508.00101* (2025).
48. Rubio, R., Ferrer, A. & Hernández, J. Preconditioning iterative solvers via the empirical interscale finite element method (eifem). *Computer Methods in Applied Mechanics and Engineering* **446**, 118257 (2025).
49. Song, J., Cao, W. & Zhang, W. A matrix preconditioning framework for physics-informed neural networks based on adjoint method. *arXiv preprint arXiv:2508.03421* (2025).
50. Zhou, X.-H. *et al.* Neural operator-based super-fidelity: A warm-start approach for accelerating steady-state simulations. *Journal of Computational Physics* **529**, 113871 (2025).
51. Eshaghi, M. S. *et al.* Multi-head neural operator for modelling interfacial dynamics. *arXiv preprint arXiv:2507.17763* (2025).

Acknowledgement

The authors would like to acknowledge the support provided by the German Academic Exchange Service (DAAD) through a scholarship awarded to Mohammad Sadegh Eshaghi during this research, as well as the Compute Servers of TU Ilmenau for providing computational resources.

Competing interests

The authors declare that they have no known competing financial interests or personal relationships that could have appeared to influence the work reported in this paper.

Figures

Fig. 1. Workflow of the Neural Operator Warm Start (NOWS) framework. Schematic overview of the NOWS methodology integrating neural operators and numerical solvers. The left branch illustrates the *data creation phase*, where data are generated, if needed (not for PI versions), using traditional solvers. The middle part describes *training phase*, where a Neural Operator is trained through a combination of data, physics, and boundary losses. The architecture cycles through lifting, integral kernels (Fourier layers), activation, and projection steps until convergence. The right branch shows the *inference phase*, in which parametric PDE problems are discretized (e.g., using FEM, IGA, FVM). The trained Neural Operator provides an initial guess for a conventional iterative solver (e.g., CG, GMRES), which then refines the solution to full numerical accuracy. This hybrid workflow leverages the efficiency of learned models and the robustness of classical solvers to accelerate PDE solvers.

Fig. 2. NOWS accelerates iterative solvers in various resolutions. (a) Overlaid residual-vs-iteration trajectories for the two methods on the 2000-sample test set, showing that NOWS reduces both the initial residual and the number of iterations to convergence. (b) Violin plots of wall-clock time distributions (per test instance) required to reach several relative residual tolerances, comparing the baseline and NOWS. (c) An example test case comparing the NOWS solution, the reference obtained with the direct solver. The NOWS removes the large-scale error, while the classical solver enforces exactness. Results are aggregated over 2000 unseen GRF realizations.

Fig. 3. Impact of physics-informed training and neural-operator warm starts (NOWS) on Darcy flow simulations. (a) Test error as a function of network complexity, comparing data-only, physics-only, and hybrid training strategies. Physics-informed supervision yields the most robust generalization, with test error decreasing as the number of Fourier modes or network parameters increases, whereas data-only and hybrid approaches exhibit overfitting. Embedding the PDE directly in the loss produces smoother and more stable operator predictions that respect the underlying physics across resolutions and heterogeneous permeability contrasts. (b) Wall-clock runtime distributions for various preconditioners and relative tolerance levels, with and without NOWS initialization. Across all preconditioners, NOWS consistently reduces solver runtime, demonstrating measurable acceleration even for simple Jacobi preconditioning, with more pronounced improvements for ICC and ILU schemes. (c) Relative residuals versus iteration count for different preconditioners. NOWS systematically lowers the initial residual and reduces the number of iterations required to achieve the prescribed convergence tolerance, illustrating solver-agnostic acceleration and robustness across preconditioning strategies.

Fig. 4. NOWS accelerates the iterative solution of PDEs on irregular domains. (a) Random samples of allowable domain configurations with arbitrary voids. The plate is clamped on the left edge and subjected to constant traction on the right edge. (b) Relative residuals versus iteration count for the conjugate gradient (CG) solver initialized from zero or using the neural operator warm start (NOWS). NOWS consistently reduces the initial residual magnitude, lowering the convergence curve and decreasing the number of iterations required to reach the target tolerance. (c) Wall-clock runtime to convergence for 50 test instances. Across all geometries, NOWS yields 10-fold speed-up and reduces iteration counts by roughly 90%. Annotated percentages indicate the fraction of computational time saved, demonstrating robust acceleration benefits even for complex domain configurations.

Fig. 5. NOWS for dynamic problems (a) Ensemble of initial conditions in the test dataset used for the Burgers' equation. (b) Comparing runtime distributions of CG and NOWS: scatter plot of runtime versus L_2 error for each sample (top), violin plots comparing the runtime distributions of the CG and NOWS solvers (bottom). (c) Spatiotemporal evolution of the solution field for a representative test sample in the Burgers' equation: exact reference (top), NOWS result (middle), and the corresponding error field (bottom). (d) **Resolution-invariant acceleration of coupled fluid–smoke simulations using NOWS.** A rising smoke plume governed by buoyancy-driven Navier–Stokes dynamics is simulated using NOWS. The neural operator, trained on coarse 64×64 grids, is applied directly to 256×256 simulations without retraining. Shown are representative smoke density snapshots at multiple time steps, illustrating stable and accurate evolution. The NOWS initialization reduces total solver iterations by over 70% and accelerates runtime by a factor of three, confirming robust resolution-invariant generalization across grid scales.